

Contents

List of Figures	ii
1 Theory	1
1.1 Introduction	1
1.2 Unit processes	3
1.2.1 Initial-value line	3
1.2.2 Internal point	4
1.2.3 Point on axis	6
1.2.4 Wall point - Direct method	6
1.2.5 Wall point - Inverse method	8
1.2.6 Free pressure point	10
1.3 Solution strategy	12
1.3.1 Parameters	12
1.3.2 Extent of the initial-value problem	13
1.3.3 Extent of the flow field determined by the initial-expansion contour	14
1.3.4 Complete flow field determined by the nozzle contour	14
1.3.5 Extent of the plume	16
1.4 Results	17
Bibliography	20

List of Figures

1.1	Schematic illustration of the geometry of the nozzle.	2
1.2	Schematic illustration of the characteristics in the two-dimensional space.	3
1.3	Nozzle throat geometry and coordinate system for transonic flow analysis and initial-value line $v = 0$	4
1.4	Schematic illustration of the characteristics in the two-dimensional space.	5
1.5	Schematic illustration of the characteristics in the two-dimensional space in the case of a point located on the axis of symmetry.	7
1.6	Schematic illustration of the characteristics in the two-dimensional space in the case of a point located on the wall, direct method.	7
1.7	Schematic illustration of the characteristics in the two-dimensional space in the case of a point located on the wall, inverse method.	9
1.8	Schematic illustration of the characteristics in the two-dimensional space in the case of a point located on free-pressure boundary.	11
1.9	Extent of the initial-value line.	13
1.10	Extent of the flow field determined by the initial-expansion contour.	14
1.11	Extent of the flow field determined by the nozzle contour and enlargement to highlight the crossing characteristics.	15
1.12	Continuous Prandtl-Meyer expansion wave.	16
1.13	Extent of the plume outside of the nozzle. Static pressure ratio = 2.	17
1.14	Mach number, static temperature [K], velocity magnitude [m/s] and flow direction [deg] inside the nozzle and plume for a static pressure ratio $p_e/p_0 = 2$	18
1.15	Mach number and ratio static pressure / stagnation pressure on the wall, the axis and 1D theory.	19

Chapter 1

Theory

1.1 Introduction

The present code solves the two-dimensional supersonic flow inside a nozzle. The shape of the nozzle is supposed to be known. Thus this code does not aim at designing a nozzle from desired requirements at the exit. Moreover the flow is steady and irrotational. The nozzle can be switched from planar to axisymmetric through a single parameter. The numerical method used in the code is a method of characteristics (MOC). This method offers the most accurate results among the marching-type numerical methods. The reader is referred to the two-volume books *Gas Dynamics* by Zucrow and Hoffman [1] for detailed explanations on the physics and the numerical method implemented. It also looks like a similar project has been implemented in the Master theses of Morham [2] and Massman [3]. These works focussed on the planar / axisymmetrical flows encountered in an ejector, which mixes a primary supersonic flow and a secondary entrained subsonic flow. The geometric restriction of the ejector induces an iterative computation for solving the primary flow and its plume with a MOC and the secondary flow with standard isentropic relations along with stagnation properties and the shape of the primary plume.

Figure 1.1 provides an overview of the geometry of the nozzle. Only the supersonic part of the flow is of interest. Moreover it is supposed that a sonic condition is met at the throat of the nozzle. As a consequence only the region downstream of the throat is kept. The throat contour is joined tangentially to a second-order polynomial. The required geometric data are

- y_t the nozzle throat radius
- ρ_{tu} the radius of curvature of the upstream circular arc at the throat
- ρ_{td} the radius of curvature of the downstream circular arc at the throat
- θ_a the attachment angle between the downstream circular arc and the 2nd-order polynomial
- θ_e the exit lip angle
- x_e the nozzle length

The governing equations for steady two-dimensional irrotational flow are

$$(u^2 - a^2) u_x + (v^2 - a^2) v_y + 2uvu_y - \delta \frac{a^2 v}{y} = 0 \quad (1.1)$$

$$u_y - v_x = 0 \quad (1.2)$$

$$a = a(u, v) = \sqrt{\gamma RT - (\gamma - 1)(u^2 + v^2)/2} \quad (1.3)$$

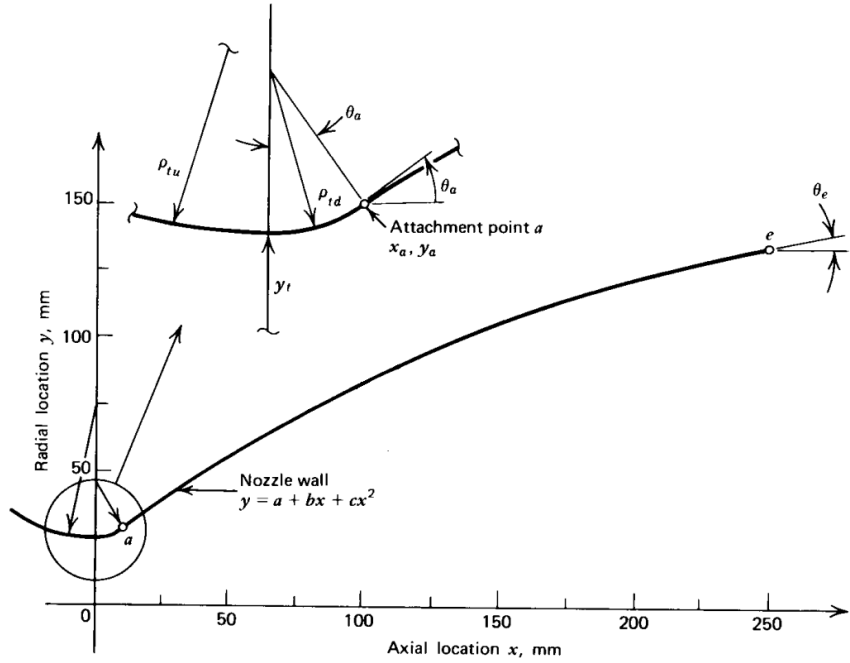


Figure 1.1: Schematic illustration of the geometry of the nozzle.

where (u, v) are the velocity components along the x - and y -directions respectively. a is the sonic speed and is a function of (u, v) only. T is the stagnation temperature, P is the stagnation pressure, R is the gas constant and γ is the ratio of specific heats. $\delta = 0$ for planar flows and $\delta = 1$ for axisymmetric flows. The subscripts x and y denote the partial derivative along the specified direction. The Mach number M is a function of the sonic speed a and the magnitude of the velocity:

$$M = a\sqrt{u^2 + v^2} \quad (1.4)$$

The static pressure p , static temperature t and density ρ are then evaluated by the relations

$$p = \frac{P}{\left(1 + \frac{\gamma-1}{2}M^2\right)^{\frac{\gamma}{\gamma-1}}} \quad (1.5a)$$

$$t = \frac{T}{\left(1 + \frac{\gamma-1}{2}M^2\right)} \quad (1.5b)$$

$$\rho = \frac{p}{Rt} \quad (1.5c)$$

The characteristic and compatibility equations corresponding to the governing equations are given by

Characteristic equation

$$\left(\frac{dy}{dx}\right)_\pm = \lambda_\pm = \tan(\theta \pm \alpha) \quad (1.6)$$

Compatibility equation

$$(u^2 - a^2) du_\pm + (2uv - (u^2 - a^2)) dv_\pm - \delta \frac{a^2 v}{y} dx_\pm = 0 \quad (1.7)$$

Figure 1.2 illustrates the C_+ and C_- characteristics and the angles θ and α . The \pm in the previous equations correspond to the C_+ and C_- characteristics respectively. The subscript \pm means that the differentials dx , du and dv are determined along the C_+ and C_- characteristics.

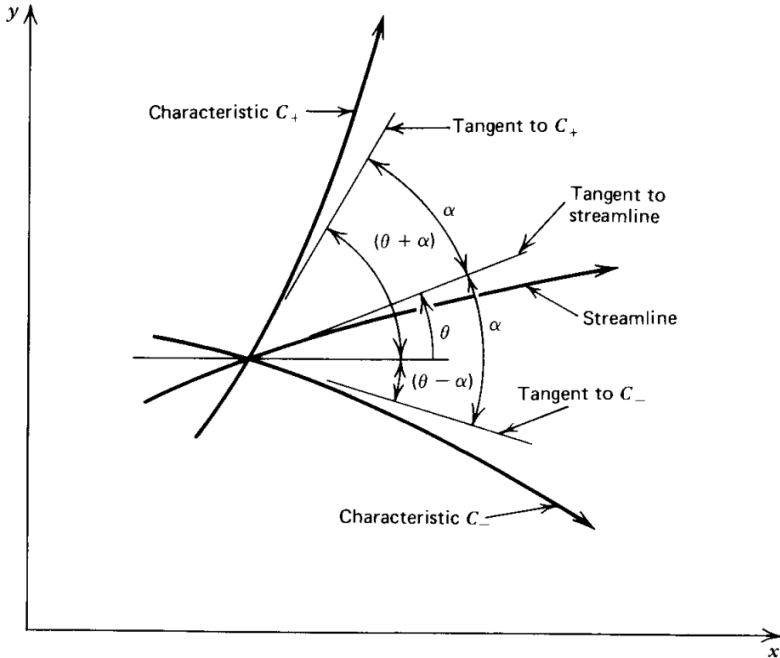


Figure 1.2: Schematic illustration of the characteristics in the two-dimensional space.

1.2 Unit processes

The method of characteristics is a marching-type numerical method. An initial-value line is thus required in order to find out the data in the domain downstream from that initial-value line. This line is prescribed in the throat region, where the flow is supersonic. Details about this line follow in Section 1.2.1.

Equations (1.6) and (1.7) are discretized in a finite difference form by a modified Euler predictor-corrector method. Sections 1.2.2 - 1.2.5 detail the implementation to determine the solution at an internal point, on the axis and on the wall.

1.2.1 Initial-value line

The MOC is based on hyperbolic equations. Such problems propagate information from an initial-value point/line/surface towards the downstream direction, following the direction of the characteristics. Information can not propagate upstream, against the direction of the velocity. An initial-value line is thus required at the throat region. The initial-value line retained for the characteristic method is the locus for $v = 0$. Along this line the Mach number $M > 1$, which is a requirement for the method of characteristics. Figure 1.3 depicts the Mach line $M = 1$ and the initial-value line $v = 0$. The latter is located downstream of the line $M = 1$.

In the following ϵ is the origin of the coordinate system in the nozzle. This shifting value is equal to

$$\epsilon = -\frac{(\gamma + 1)\alpha y_t^2}{2(3 + \delta)} \quad (1.8)$$

where α is a constant (termed the coefficient of the linear non-dimensional axial perturbation velocity).

$$\alpha = \sqrt{\frac{1 + \delta}{(\gamma + 1)\rho_{tu}y_t}} \quad (1.9)$$

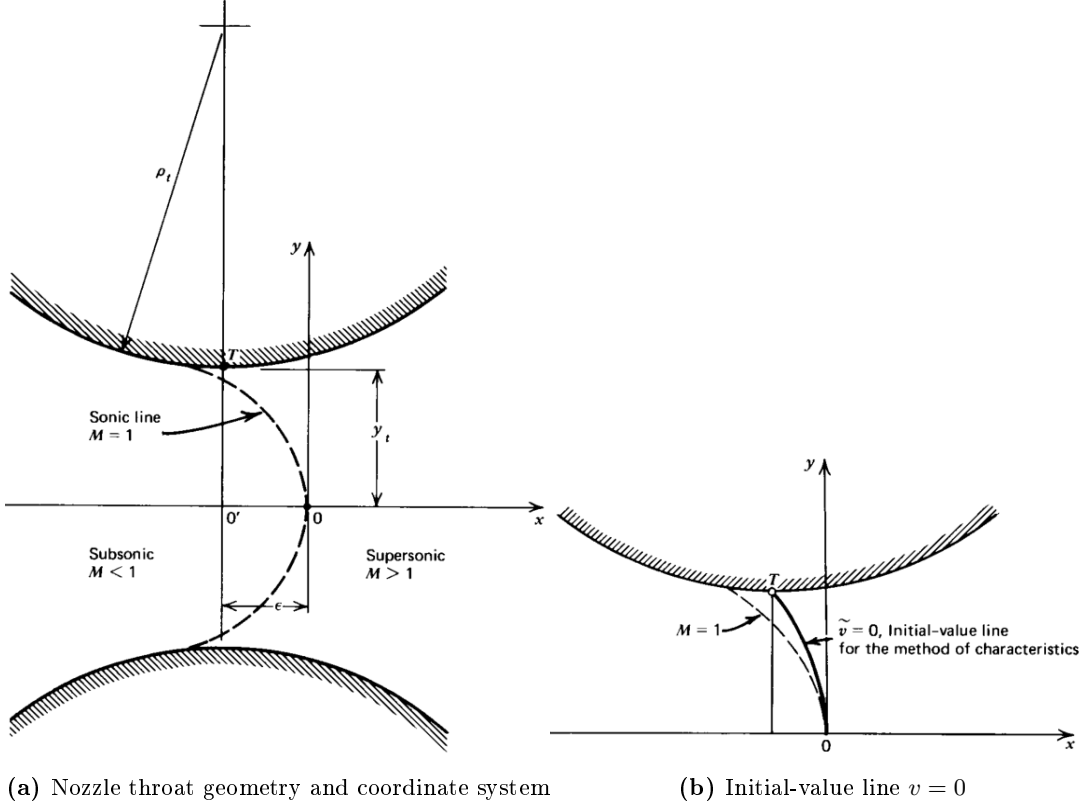


Figure 1.3: Nozzle throat geometry and coordinate system for transonic flow analysis and initial-value line $v = 0$.

The equation of the line $v = 0$ for $0 \leq y \leq y_t$ in the frame of reference specified in Fig.1.3b is

$$x = -\frac{(\gamma + 1)\alpha y^2}{2(3 + \delta)} \quad (1.10)$$

Along this line the u -velocity component is initiated to the value

$$u(x, y) = \alpha x + \frac{(\gamma + 1)\alpha^2 y^2}{2(1 + \delta)} \quad (1.11)$$

The flow being isentropic the sonic speed is function of the magnitude of the velocity $a = a(u, v)$:

$$a(u, v) = \sqrt{\gamma RT - (\gamma - 1)(u^2)/2} \quad (1.12)$$

Knowing the sonic speed and the velocity magnitude, the Mach number is easily calculated with Eq. (1.4). The static thermodynamic properties are then computed through the relations (1.5).

The x-coordinate must be corrected by the shifting ϵ in order to match the global system of coordinates centered at the throat (see Fig.1.1):

$$x_{\text{nozzle}} = x - \epsilon \quad (1.13)$$

1.2.2 Internal point

Figure 1.4 summarizes the situation. The solution is known at points 1 and 2 and must be calculated at point 4. For this purpose one computes the intersection between the left-running

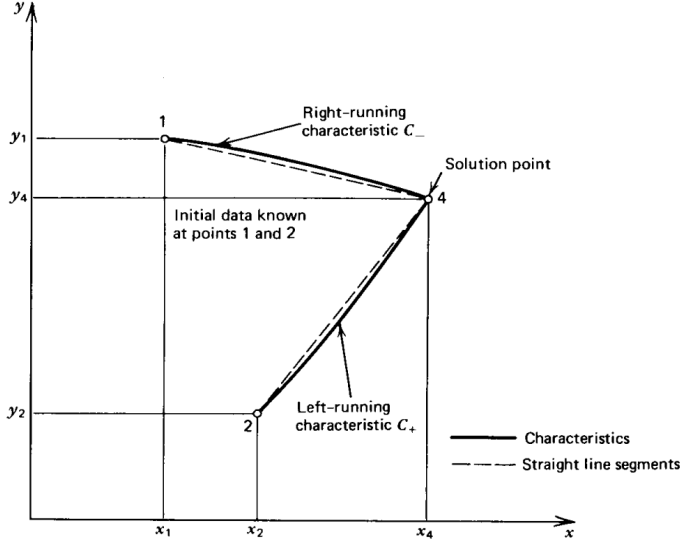


Figure 1.4: Schematic illustration of the characteristics in the two-dimensional space.

characteristic C_+ emanating from point 2 and the right-running characteristics C_- emanating from point 1.

A first location of the intersection is estimated by assuming that the two characteristics are straight line segments. This allows to determine a first estimation of the solution at point 4. This first step is termed the predictor step. A better guess for the location of point 4 is then iteratively determined by averaging the solution of nodes 2 and 4. This is the corrector step. Equations (1.6) and (1.7) are discretized at points 1, 2 and 4 for this purpose. The following steps solved to get the location and solution at point 4:

$$\theta_{\pm} = \tan^{-1} \left(\frac{v_{\pm}}{u_{\pm}} \right) \quad (1.14a)$$

$$V_{\pm} = \sqrt{u_{\pm}^2 + v_{\pm}^2} \quad (1.14b)$$

$$a_{\pm} = a(u_{\pm}, v_{\pm}) \quad (1.14c)$$

$$\alpha_{\pm} = \sin^{-1} \left(\frac{a_{\pm}}{V_{\pm}} \right) \quad (1.14d)$$

$$\lambda_{\pm} = \tan(\theta_{\pm} \pm \alpha_{\pm}) \quad (1.14e)$$

$$Q_{\pm} = u_{\pm}^2 - a_{\pm}^2 \quad (1.14f)$$

$$R_{\pm} = 2u_{\pm}v_{\pm} - Q_{\pm}\lambda_{\pm} \quad (1.14g)$$

$$S_{\pm} = \delta \frac{a_{\pm}^2 v_{\pm}}{y_{\pm}} \quad (1.14h)$$

The definition of the sonic speed a_{\pm} is given in Eq. (1.1). The location of point 4 emerges from the solving of

$$\begin{pmatrix} -\lambda_+ & 1 \\ -\lambda_- & 1 \end{pmatrix} \begin{pmatrix} x_4 \\ y_4 \end{pmatrix} = \begin{pmatrix} y_2 - \lambda_+ x_2 \\ y_1 - \lambda_- x_1 \end{pmatrix} \quad (1.15)$$

The velocity components at point 4 are then calculated by solving

$$\begin{pmatrix} Q_+ & R_+ \\ Q_- & R_- \end{pmatrix} \begin{pmatrix} u_4 \\ v_4 \end{pmatrix} = \begin{pmatrix} S_+(x_4 - x_2) + Q_+ u_2 + R_+ v_2 \\ S_-(x_4 - x_1) + Q_- u_1 + R_- v_1 \end{pmatrix} \quad (1.16)$$

1.2.2.1 Predictor step

As a first step the values for the flow properties u_{\pm} , v_{\pm} and y_{\pm} are set equal to their values at points 2 and 1 respectively. This provides a first estimation of the location for point 4 (x_4^0, y_4^0) and the velocity (u_4^0, v_4^0) at this point. This initial estimation then feeds the corrector step.

1.2.2.2 Corrector step

Each corrector step follows the same steps as described above except that the values are averaged between points 1, 2 and 4:

$$x_- = x_1 \quad x_+ = x_2 \quad (1.17)$$

$$y_- = \frac{y_1 + y_4}{2} \quad y_+ = \frac{y_2 + y_4}{2} \quad (1.18)$$

$$u_- = \frac{u_1 + u_4}{2} \quad u_+ = \frac{u_2 + u_4}{2} \quad (1.19)$$

$$v_- = \frac{v_1 + v_4}{2} \quad v_+ = \frac{v_2 + v_4}{2} \quad (1.20)$$

This provides the values for (x_4^n, y_4^n) and the velocity (u_4^n, v_4^n) , which are required to estimate the solution (x_4^{n+1}, y_4^{n+1}) and the velocity (u_4^{n+1}, v_4^{n+1}) at the next iteration level. The iterative process is stopped once the difference in the position and velocity is smaller than a threshold or when the number of iterations exceeds a maximum value.

Function MOC_2D_steady_irrotational_internal_point.m implements the algorithm detailed hereabove.

1.2.3 Point on axis

The case where point 4 is located on the axis of symmetry is a particularization of the previous section. Indeed one sees on Fig. 1.5 that point 2 is located outside of the computational domain and is the mirror image of point 1. An additional constraint is that $y_4 = v_4 = \theta_4 = 0$. Thus the same algorithm is used as in the previous section, with the specification that $x_2 = x_1$, $y_2 = -y_1$, $u_2 = u_1$ and $v_2 = -v_1$.

1.2.4 Wall point - Direct method

At the wall point 4 the direction of the velocity vector must be identical to the local slope of the wall (see Fig. 1.6). The direct method makes no assumption on the location of the wall point and extends *directly* the C_+ characteristic from the known interior point 2 until it meets the wall. Point 1 does not exist in this case. The characteristic and compatibility equations from the C_+ are completed by two additional conditions for determining the location and flow properties at point 4:

$$y_4 = y(x_4) \quad \text{specified on the wall} \quad (1.21)$$

$$\frac{dy}{dx} = \tan(\theta_4) = \frac{v_4}{u_4} \quad \text{specified on the wall} \quad (1.22)$$

The geometry of the nozzle is discussed in section 1.1 but can be modified at wish in function MOC_2D_steady_irrotational_get_geometry.m. This function returns the ordinate y and the slope of the wall at a specified abscissae x and the values of the coefficients a , b and c for the second-order polynomial $y = a + bx + cx^2$.

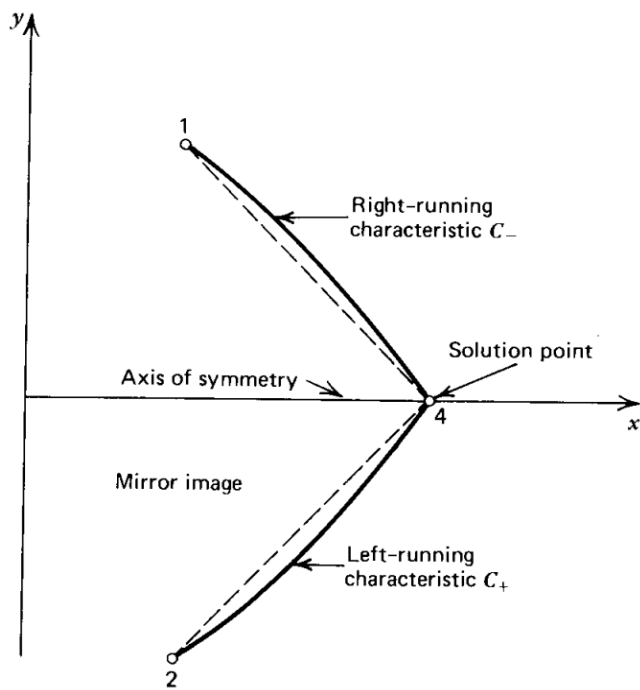


Figure 1.5: Schematic illustration of the characteristics in the two-dimensional space in the case of a point located on the axis of symmetry.

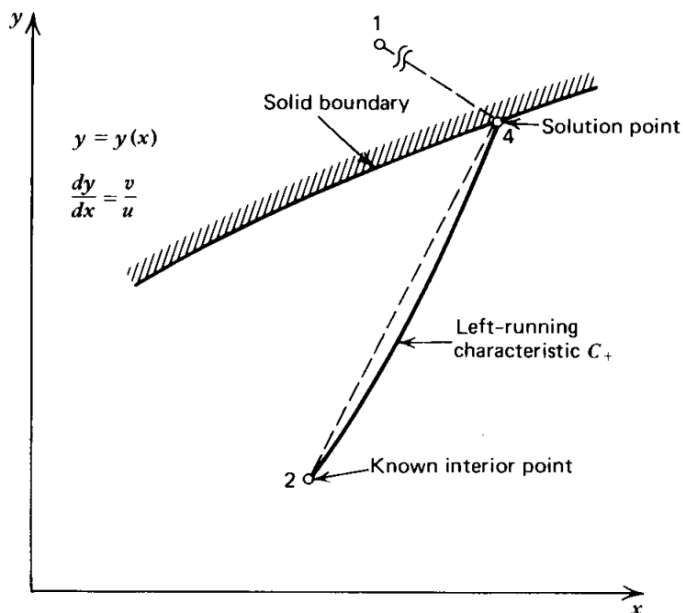


Figure 1.6: Schematic illustration of the characteristics in the two-dimensional space in the case of a point located on the wall, direct method.

Equations (1.14) can be reused to obtain the parameters of the left-running characteristic C_+ . The location of point 4 (x_4, y_4) is obtained by intersecting the C_+ characteristic and the 2nd-order polynomial:

$$y_4 = \lambda_+ x_4 + y_2 - \lambda_+ x_2 \quad (1.23)$$

$$y_4 = a + bx_4 + cx_4^2 \quad (1.24)$$

which gives the only acceptable solution

$$x_4 = \frac{\lambda_+ - b - \sqrt{(\lambda_+ - b)^2 - 4c(a - y_2 + \lambda_+ x_2)}}{2c} \quad (1.25)$$

In the particular case where $c = 0$ (i.e. $\theta_a = \theta_e$, the nozzle is a straight line), then

$$x_4 = \frac{a - y_2 + \lambda_+ x_2}{\lambda_+ - b} \quad (1.26)$$

The velocity components at point 4 are then calculated by solving

$$\begin{pmatrix} Q_+ & R_+ \\ b + 2cx_4 & -1 \end{pmatrix} \begin{pmatrix} u_4 \\ v_4 \end{pmatrix} = \begin{pmatrix} S_+(x_4 - x_2) + Q_+ u_2 + R_+ v_2 \\ 0 \end{pmatrix} \quad (1.27)$$

1.2.4.1 Predictor step

As a first step the values for the flow properties u_+ , v_+ and y_+ are set equal to their values at points 2. This provides a first estimation of the location for point 4 (x_4^0, y_4^0) and the velocity (u_4^0, v_4^0) at this point. This initial estimation then feeds the corrector step.

1.2.4.2 Corrector step

Each corrector step follows the same steps as described above except that the values are averaged between points 2 and 4:

$$x_+ = x_2 \quad (1.28)$$

$$y_+ = \frac{y_2 + y_4}{2} \quad (1.29)$$

$$u_+ = \frac{u_2 + u_4}{2} \quad (1.30)$$

$$v_+ = \frac{v_2 + v_4}{2} \quad (1.31)$$

This provides the values for (x_4^n, y_4^n) and the velocity (u_4^n, v_4^n) , which are required to estimate the solution (x_4^{n+1}, y_4^{n+1}) and the velocity (u_4^{n+1}, v_4^{n+1}) at the next iteration level. The iterative process is stopped once the difference in the position and velocity is smaller than a threshold or when the number of iterations exceeds a maximum value.

Function MOC_2D_steady_irrotational_wall.m implements the algorithm detailed here-above.

1.2.5 Wall point - Inverse method

The previous section focussed on the case where the location of the wall point is found by extending the characteristic from an internal point. This method can lead in too sparse wall points in regions where the gradients are extremely large. One can resort to the inverse wall point

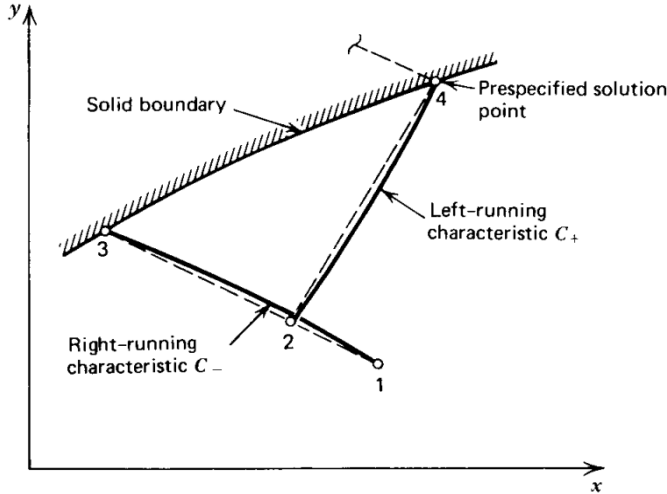


Figure 1.7: Schematic illustration of the characteristics in the two-dimensional space in the case of a point located on the wall, inverse method.

method to prespecify spatial spacing along the wall and employing the method of characteristics for computing the flow properties at the prespecified wall points.

This is illustrated in Fig. 1.7. Points 1 and 3 are known from previous calculations, point 4 is the prespecified wall point and point 2 is the intersection between the right-running characteristic C_- 13 and the left-running characteristic C_+ emanating from point 4. The flow properties at point 2 are then interpolated between points 1 and 3. The flow properties at point 4 are determined with the first line of the system of equations (1.16) and the condition (1.22).

The slope of the characteristic 24 depends on the unknown flow properties at points 2 and 4. A predictor-corrector method is thus required to locate point 2 during each step of the global modified Euler predictor-corrector algorithm:

- Initialize (x_+, y_+, u_+, v_+) , see the next subsections on the global predictor and corrector steps.
- While the values (x_2, y_2, u_2, v_2) did not converge, do the following steps:

$$\theta_+ = \tan^{-1} \left(\frac{v_+}{u_+} \right) \quad (1.32)$$

$$V_2 = \sqrt{u_+^2 + v_+^2} \quad (1.33)$$

$$a_+ = a(u_+, v_+) \quad (1.34)$$

$$\alpha_+ = \sin^{-1} \left(\frac{a_+}{V_+} \right) \quad (1.35)$$

$$\lambda_+ = \tan(\theta_+ + \alpha_+) \quad (1.36)$$

$$\lambda_- = \frac{y_3 - y_1}{x_3 - x_1} \quad (1.37)$$

Solve the system of equations

$$\begin{pmatrix} -\lambda_- & 1 \\ -\lambda_+ & 1 \end{pmatrix} \begin{pmatrix} x_2 \\ y_2 \end{pmatrix} = \begin{pmatrix} y_1 - \lambda_- x_1 \\ y_4 - \lambda_+ x_4 \end{pmatrix} \quad (1.38)$$

Interpolate the data

$$\begin{pmatrix} u_2 \\ v_2 \end{pmatrix} = \begin{pmatrix} u_1 \\ v_1 \end{pmatrix} + \frac{x_2 - x_1}{x_3 - x_1} \begin{pmatrix} u_3 - u_1 \\ v_3 - v_1 \end{pmatrix} \quad (1.39)$$

- Once (x_2, y_2, u_2, v_2) have converged, compute the data at point 4:

$$Q_+ = u_2^2 - a_2^2 \quad (1.40)$$

$$R_+ = 2u_2v_2 - Q_+\lambda_+ \quad (1.41)$$

$$S_+ = \delta \frac{a_+^2 v_2}{y_2} \quad (1.42)$$

Solve the system of equations

$$\begin{pmatrix} Q_+ & R_+ \\ \tan \theta_4 & -1 \end{pmatrix} \begin{pmatrix} u_4 \\ v_4 \end{pmatrix} = \begin{pmatrix} S_+(x_4 - x_2) + Q_+u_2 + R_+v_2 \\ 0 \end{pmatrix} \quad (1.43)$$

1.2.5.1 Global predictor step

As a first step the values for the flow properties u_2 and v_2 are set equal to their values at point 3, which means $u_+ = u_3$ and $v_+ = v_3$. Following the procedure explained hereabove provides a first estimation of the location for point 2 (x_2^0, y_2^0) and the flow field $(u_2^0, v_2^0, u_4^0, v_4^0)$. This initial estimation then feeds the corrector step.

1.2.5.2 Global corrector step

Each corrector step follows the same steps as described above except that the values are averaged between points 2 and 4:

$$u_+ = \frac{u_2 + u_4}{2} \quad v_+ = \frac{v_2 + v_4}{2} \quad (1.44)$$

This provides the values for (x_2^n, y_2^n) and the flow field $(u_2^n, v_2^n, u_4^n, v_4^n)$, which are required to estimate the solution at the next iteration level. The iterative process is stopped once the difference in the position and velocity is smaller than a threshold or when the number of iterations exceeds a maximum value.

Function MOC_2D_steady_irrotational_wall_inverse.m implements the algorithm detailed hereabove.

1.2.6 Free pressure point

The last configuration is the case where point 4 is located on the free-pressure boundary (see Fig.1.8). Such a boundary appears outside of the nozzle when a compressible flow discharges into an ambient atmosphere having a static pressure p_0 . At point 4 on this boundary, the condition $p_4 = p_0$ must be taken into account in the numerical procedure. In addition to that condition one compatibility equation is available from the left-running characteristic C_+ 24. Furthermore the fluid velocity and static pressure in the jet are related only by the relationship for isentropic flows. A last relationship is required for determining the location of point 4. That relationship is given by the condition that the jet boundary is a streamline and thus

$$V_4 = \sqrt{\frac{2\gamma RT}{\gamma - 1} \left(1 - \left(\frac{p_4}{P} \right)^{\frac{\gamma-1}{\gamma}} \right)} \quad (1.45a)$$

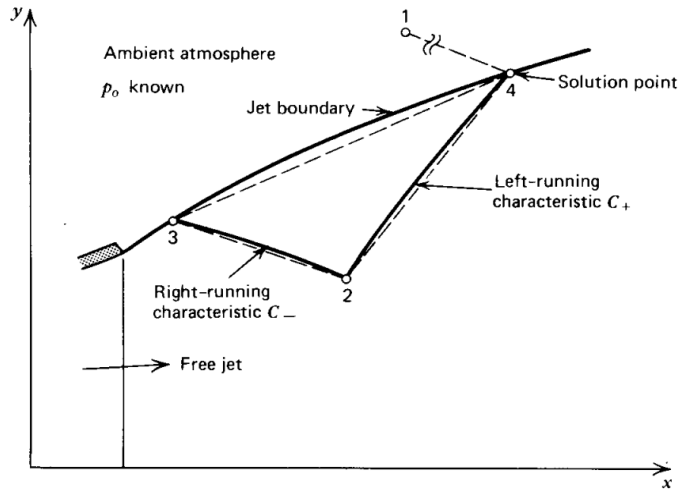


Figure 1.8: Schematic illustration of the characteristics in the two-dimensional space in the case of a point located on free-pressure boundary.

$$\theta_+ = \tan^{-1} \left(\frac{v_+}{u_+} \right) \quad (1.45b)$$

$$V_+ = \sqrt{u_+^2 + v_+^2} \quad (1.45c)$$

$$a_+ = a(u_+, v_+) \quad (1.45d)$$

$$\alpha_+ = \sin^{-1} \left(\frac{a_+}{V_+} \right) \quad (1.45e)$$

$$\lambda_+ = \tan(\theta_+ \pm \alpha_+) \quad (1.45f)$$

$$Q_+ = u_+^2 - a_+^2 \quad (1.45g)$$

$$R_+ = 2u_+v_+ - Q_+\lambda_+ \quad (1.45h)$$

$$S_+ = \delta \frac{a_+^2 v_+}{y_+} \quad (1.45i)$$

$$\lambda_0 = \frac{v_3}{u_3} \quad \text{predictor step} \quad (1.45j)$$

$$= \frac{v_3 + v_4}{u_3 + u_4} \quad \text{corrector step}$$

The definition of the sonic speed a_+ is given in Eq. (1.1). The location of point 4 emerges from the solving of

$$\begin{pmatrix} -\lambda_+ & 1 \\ -\lambda_0 & 1 \end{pmatrix} \begin{pmatrix} x_4 \\ y_4 \end{pmatrix} = \begin{pmatrix} y_2 - \lambda_+ x_2 \\ y_3 - \lambda_0 x_3 \end{pmatrix} \quad (1.46)$$

The velocity components at point 4 are then calculated by

$$T_+ = S_+(x_4 - x_2) + Q_+u_2 + R_+v_2 \quad (1.47a)$$

$$u_4 = \frac{Q_+T_+ - R_+ \sqrt{V_4^2(Q_+^2 + R_+^2) - T_+^2}}{Q_+^2 + R_+^2} \quad (1.47b)$$

$$v_4 = \sqrt{V_4^2 - u_4^2} \quad (1.47c)$$

1.2.6.1 Predictor step

As a first step the values for the flow properties u_+ , v_+ and y_+ are set equal to their values at points 2. This provides a first estimation of the location for point 4 (x_4^0, y_4^0) and the velocity (u_4^0, v_4^0) at this point. This initial estimation then feeds the corrector step.

1.2.6.2 Corrector step

Each corrector step follows the same steps as described above except that the values are averaged between points 2 and 4:

$$x_+ = x_2 \quad (1.48)$$

$$y_+ = \frac{y_2 + y_4}{2} \quad (1.49)$$

$$u_+ = \frac{u_2 + u_4}{2} \quad (1.50)$$

$$v_+ = \frac{v_2 + v_4}{2} \quad (1.51)$$

This provides the values for (x_4^n, y_4^n) and the velocity (u_4^n, v_4^n) , which are required to estimate the solution (x_4^{n+1}, y_4^{n+1}) and the velocity (u_4^{n+1}, v_4^{n+1}) at the next iteration level. The iterative process is stopped once the difference in the position and velocity is smaller than a threshold or when the number of iterations exceeds a maximum value.

Function MOC_2D_steady_irrotational_free_pressure.m implements the algorithm detailed hereabove.

1.3 Solution strategy

In this section the strategy to solve the flow field inside the nozzle and in the plume is detailed.

1.3.1 Parameters

Hereunder the parameters required to launch the simulation are summarized. Please refer to Fig.1.1 for the geometrical parameters.

```
% Parameters for the flow field
params.gamma = 1.2; % Specific heat ratio = Cp / Cv
params.R = 320; % [J/kg-K] Gas constant
params.P = 70.e5; % [Pa] Stagnation pressure
params.PRatio = 2; % Ratio of static pressure at exit lip point
% [>1 to have a Prandtl-Meyer expansion]
% PRatio = Pstatic_lip / Pstatic_ambient
params.T = 3000; % [K] Stagnation temperature

% Parameters for the geometry
geom.delta = 1; % [0/1] 0: planar nozzle
% 1: axisymmetric nozzle
geom.yt = 1.; % [m] Throat radius, used as reference length for whole nozzle
geom.rhou = 2 * geom.yt; % [m] Throat upstream radius of circular arc
geom.rhod = 0.5 * geom.yt; % [m] Throat downstream radius of circular arc
geom.xe = 10 * geom.yt; % [m] Nozzle length
geom.xplume= 20 * geom.yt; % [m] Axial length of the plume
geom.ta = 15; % [deg] Attachment angle between circular arc and line
geom.te = 15; % [deg] Exit lip point angle

% Parameters for the discretization
```

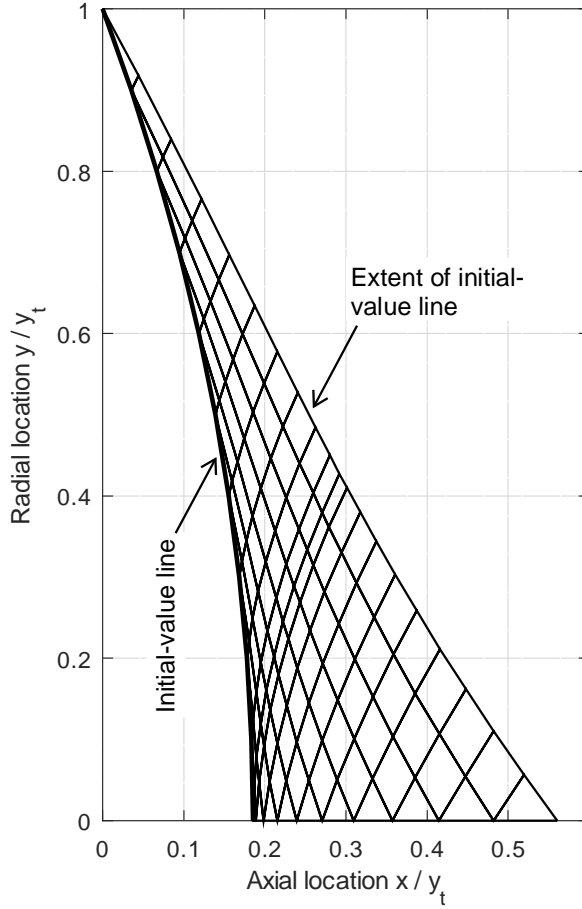


Figure 1.9: Extent of the initial-value line.

```

geom.NI      = 11;          % Number of points on the initial-value line
geom.circdownTheta = 1:1:geom.ta; % Discretization of the circ. arc downstream of throat
geom.NIexpansion = 10;        % Number of expansion waves, if any exists

% Parameters for the post-processing of the results
plots.patches = 1; % [0/1] Plot the 2D patches to visualize the characteristics and
                   % the solution inside the nozzle
plots.patches_data = 1; % 0: plot only the outlines of the patches -> no colour
                       % 1: plot the Mach number
                       % 2: the static pressure
                       % 3: the static temperature
                       % 4: the density
                       % 5: the amplitude of the velocity
plots.patches_xlim = 20 * geom.yt; % Abscissa above which the patch plot is cut

```

1.3.2 Extent of the initial-value problem

The initial-value line described in section 1.2.1 is discretized on `geom.NI` points. The computation starts at the axis and steps towards the wall point, at $y = y_t$. For each point on the initial-value line a right-running characteristic C_- is instantiated. Internal points (see section 1.2.2) are created by intersecting this C_- with left-running characteristics C_+ emerging from points on the previous C_- . The last point on the C_- lies on the axis and the procedure explained in section 1.2.3 is employed. Once all the points on the initial-value line are visited, the extent of

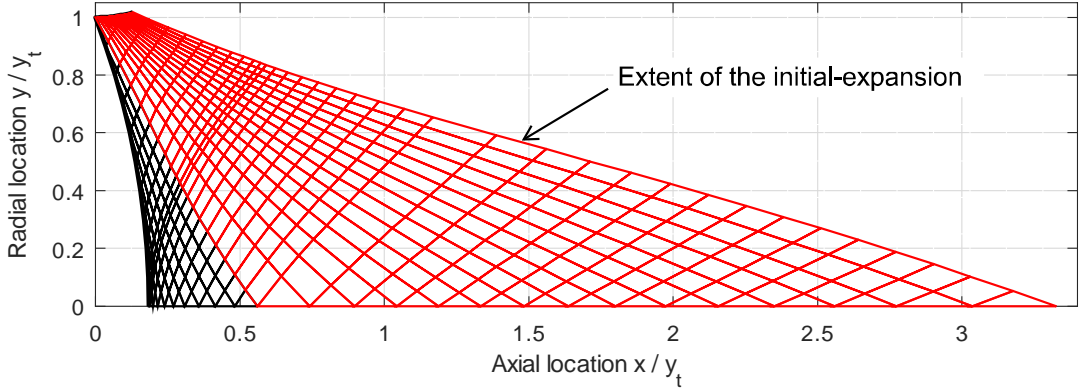


Figure 1.10: Extent of the flow field determined by the initial-expansion contour.

the initial-value line is obtained, see Fig. 1.9.

1.3.3 Extent of the flow field determined by the initial-expansion contour

In the throat region where the flow gradients are large, the direct wall point method leads to too large spacings between wall points. The inverse wall point method discussed in section 1.2.5 is used to specify wall points on the circular arc which joins the throat and the diverging section of the nozzle. The discretization of this circular arc is controlled by the parameter `geom.circdownTheta`. Once the data at a prespecified point has been determined, the right-running characteristics C_- emerging from this point is propagated inside the nozzle and internal points (see section 1.2.2) are calculated. The last point on the C_- is calculated by the axis point method (section 1.2.3). When all the prespecified wall points are visited, the extent of the initial-expansion is obtained, see Fig. 1.10.

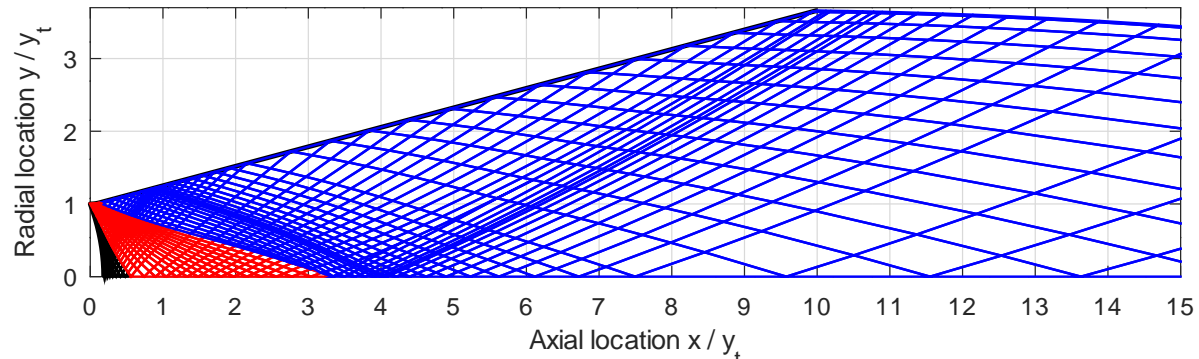
Special care must be exercised when internal points are created outside of the nozzle. This happens when C_+ characteristics from the extent of the the initial-line intersect the circular arc. Such points are deleted and the routine continues with the next C_+ characteristic.

1.3.4 Complete flow field determined by the nozzle contour

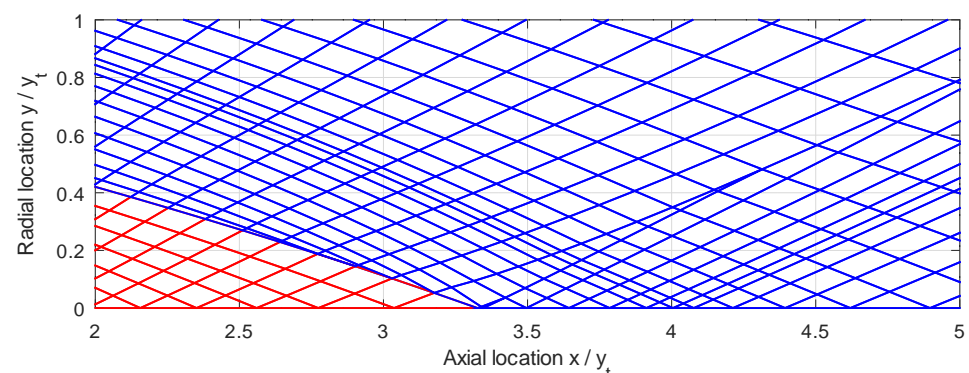
The direct wall point method (see section 1.2.4) is used to determined the wall points on the diverging section of the nozzle. Right-running characteristics C_- are then propagated towards the axis from each wall point. The procedure is repeated until the maximum axial length of the nozzle (`geom.xe`) is exceeded. The exceeding wall point is then deleted and an inverse wall point method is used to compute the data at the nozzle exit lip point. A last C_- is then propagated towards the axis. Figure 1.11 shows the pattern of the characteristics once the whole nozzle has been travelled down.

Special care must be taken for crossing characteristics of the same family. Indeed coalescing characteristics are compression waves that may steepen and form oblique shock waves. Such a coalescence is highlighted on Fig 1.11b, just downstream of the extent of the initial expansion. The reason of this compression wave is the discontinuity in wall curvature between the circular arc and the nozzle. Weak compression waves can still be managed by MOC. The computational logic of the marching procedure must however be altered. In this code the current crossing characteristic C_- is terminated and the next internal points takes the values from the previous C_- .

The reflection of the compression wave on the axis must also be treated. This reflection creates crossing left-running characteristics C_+ . When such crossings happen the current point



(a)



(b) Enlargement to highlight the crossing characteristics

Figure 1.11: Extent of the flow field determined by the nozzle contour and enlargement to highlight the crossing characteristics.

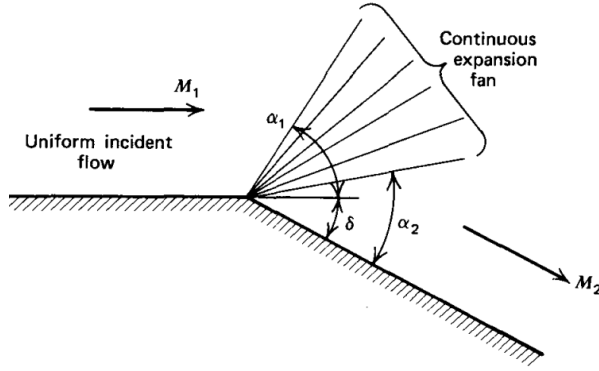


Figure 1.12: Continuous Prandtl-Meyer expansion wave.

is deleted and the routine continues with the next C_+ .

1.3.5 Extent of the plume

The extent of the flow field outside of the nozzle is maybe one of the most complex situation to handle. Indeed the ambient static pressure p_0 must be satisfied on the jet boundary (see section 1.2.6). Except in very rare cases this ambient static pressure is not achieved at the nozzle exit lip point, where at static pressure p_e is obtained. Two cases are possible:

- When $p_e > p_0$ (under-expanded nozzle) a Prandtl-Meyer expansion wave appears at the nozzle exit lip point to equalize the pressure. This expansion wave is discretized by geom.NIexpansion turning angles, as depicted on Fig. 1.12. The known data are the static pressure at the exit lip point, before the expansion wave, $p_e = p_1$ and the Mach number $m_e = M_1$. The unknowns are the deflection angle δ and the Mach number after the expansion wave M_2 . The deflection angle

$$\delta = \nu_2 - \nu_1 \quad (1.52)$$

is function of the Prandtl-Meyer deflection angle ν , which is evaluated through the following expression

$$\pm\nu = \sqrt{\frac{\gamma+1}{\gamma-1}} \tan^{-1} \left(\frac{\gamma-1}{\gamma+1} (M^2 - 1) \right) - \tan^{-1} \sqrt{M^2 - 1} \quad (1.53)$$

The + sign means a counter-clockwise deflection, which is the case in the present work. A first guess is made on the deflection angle δ . On the basis of this value, one can extract the Mach number M_2 from Eq.(1.53). This allows the calculation of the static pressure p_2 as the stagnation pressure is known (see Eq.(1.5)). On the basis of this guessed static pressure p_2 , one can iterate on the deflection angle until the condition $p_2 = p_a$ is met. The expansion fan is discretized by geom.NIexpansion lines tilted by a fraction of δ and are associated to right-running characteristics C_- emanating from the exit lip point. The standard procedure is applied for internal nodes within this expansion fan (see section 1.2.2). Once the expansion fan has been completely determined, the free-pressure point method (section 1.2.6) is applied to determine the next point on the boundary of the nozzle jet. From this point a right-running C_- is then propagated downstream until the axis is met.

- When $p_e < p_0$ (over-expanded nozzle) an oblique shock wave propagates from the exit lip point towards the axis. Because an oblique shock wave is stronger than a Mach wave, the

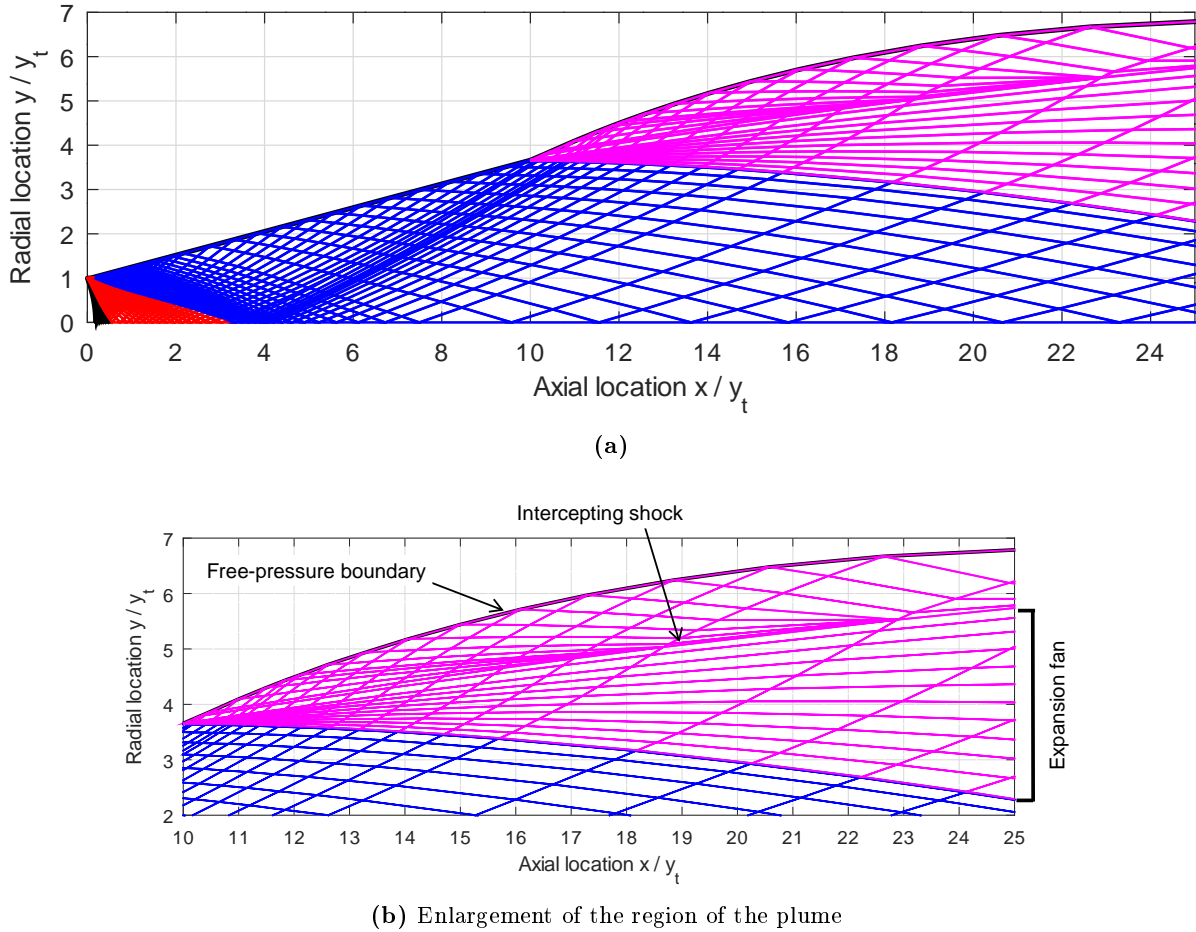


Figure 1.13: Extent of the plume outside of the nozzle. Static pressure ratio = 2.

oblique shock wave is steeper than the last right-running characteristic from the nozzle exit lip point. This implies that the flow field upstream of the last C_- must be recalculated to take into account the oblique shock wave. This strategy has not been implemented in the code yet.

The parameter `params.PRatio` takes the ratio of static pressures p_e/p_0 as value. The case $p_e/p_0 < 1$ is not implemented yet, so that only Prandtl-Meyer expansion waves are taken into account for the moment. Figure 1.13 shows the extent of the plume in the case of a pressure ratio of 2. The free-pressure boundary forms a concave curve. As a consequence right-running characteristics emanating from the free-pressure boundary intersect and gradually form an oblique shock wave. This shock wave, denoted intercepting shock, is detached from the boundary. This intercepting shock wave appears after the expansion fan, which must not be recomputed.

1.4 Results

Figure 1.14 shows the Mach number, the static temperature, the velocity magnitude and the flow direction compared to the axial direction inside the nozzle and the plume for the parameters provided in section 1.3.1. The expending nozzle has a conical shape of half-angle $\theta_e = 15\text{deg}$. The accelerating effect of the nozzle is clearly visible. One also observe the weak oblique shock generated inside the nozzle and its reflection on the axis. The intercepting shock wave inside

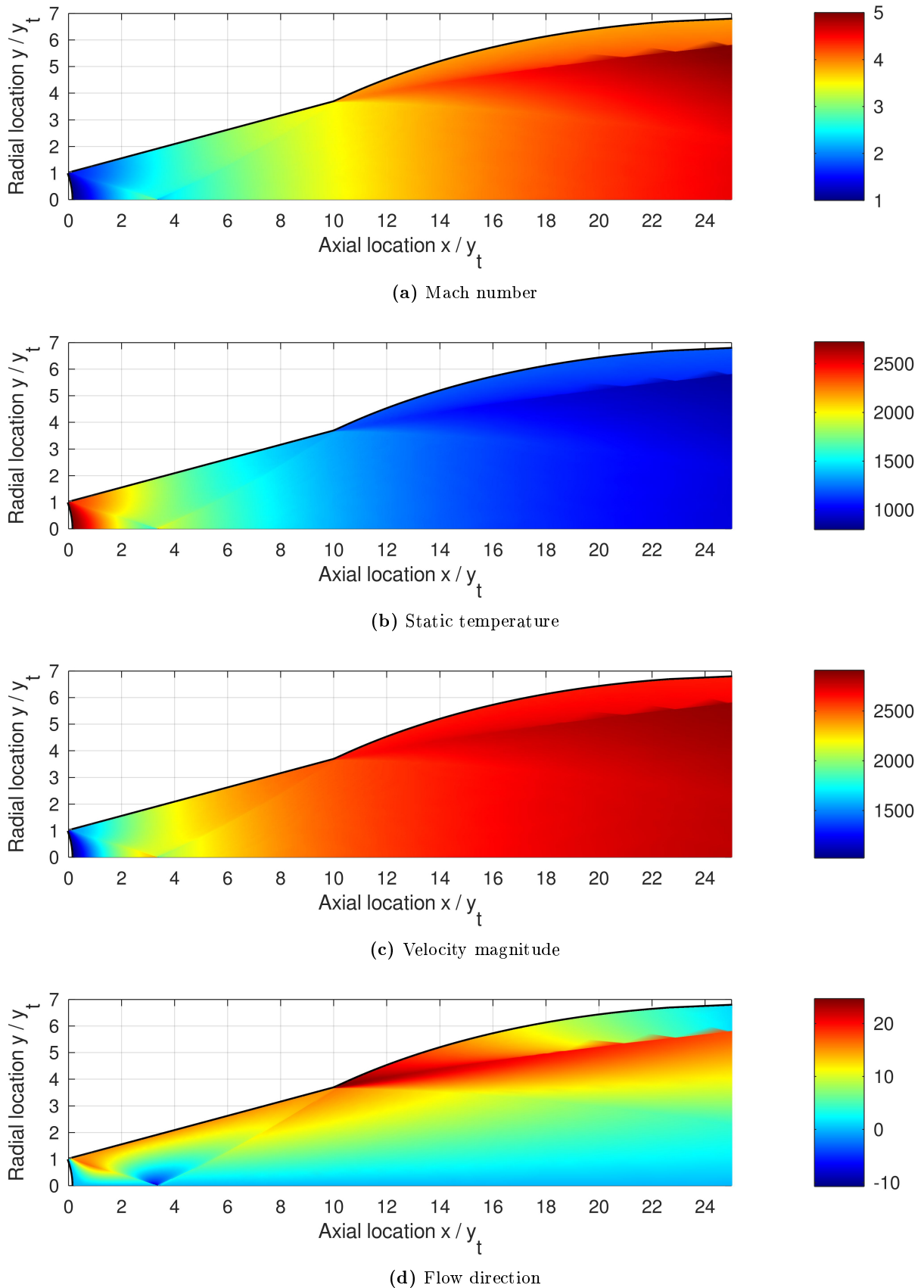


Figure 1.14: Mach number, static temperature [K], velocity magnitude [m/s] and flow direction [deg] inside the nozzle and plume for a static pressure ratio $p_e/p_0 = 2$.

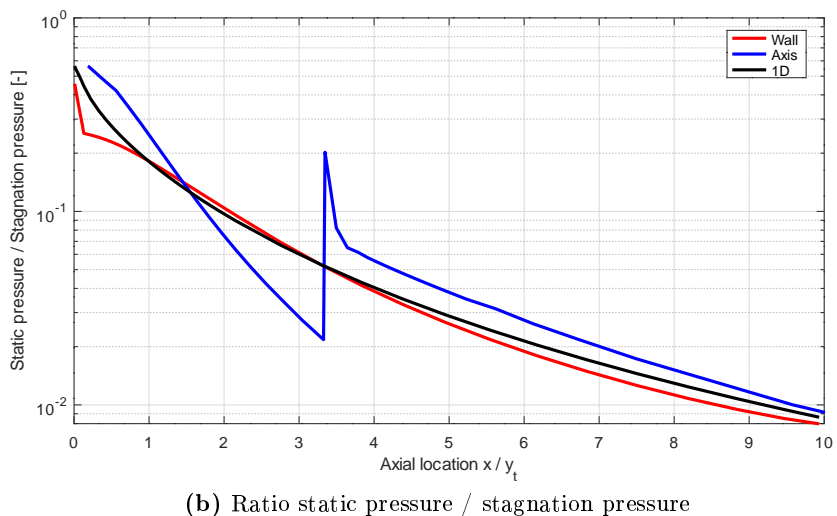
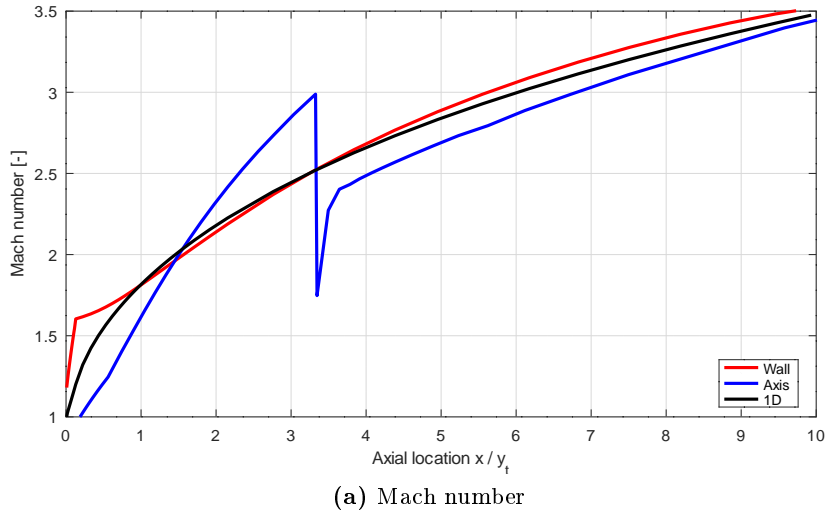


Figure 1.15: Mach number and ratio static pressure / stagnation pressure on the wall, on the axis and from 1D theory.

the plume is also quite evident. The flow direction changes across the oblique shock wave as expected.

Figure 1.15 shows the 1D evolution of the Mach number and the ratio of static pressure to stagnation pressure on the wall of the nozzle, on the axis and from the 1D theory. Inside the initial expansion region, the static pressure along the wall is considerably smaller than the 1D value, whereas the value on the axis is considerable higher. Near $x/y_t = 1.5$ downstream from the throat the three curves intersect and the static pressure on the axis drops. The reflection of the oblique shock wave on the axis occurs at around $x/y_t = 3.3$ and causes a sudden increase in static pressure on the axis. The three curves then converges towards the nozzle exit plane.

Bibliography

- [1] Zucrow, Maurice J. and Hoffman, Joe D., Gas Dynamics Volume 2: Multidimensional Flow, John Wiley and Sons, 1977.
- [2] Morham, Brett G., Numerical examination of flow field characteristics and Fabri chocking 2D supersonic ejectors, Master Thesis, California Polytechnic State University, San Luis Obispo, United States of America, 2010.
- [3] Massman, Jeffrey Alan, Numerical flow field analysis of an air augmented rocket using the ax-isymmetric method of characteristics, Master Thesis, California Polytechnic State University, San Luis Obispo, United States of America, 2013.